Bioactive Materials 6 (2021) 3596–3607

Contents lists available at ScienceDirect

Bioactive Materials

journal homepage: www.sciencedirect.com/journal/bioactive-materials

Biomimetic injectable hydrogel microspheres with enhanced lubrication and controllable drug release for the treatment of osteoarthritis

Ying Han [a,1], Jielai Yang [b,1], Weiwei Zhao [a], Haimang Wang [a], Yulong Sun [a], Yuji Chen [a], Jing Luo [c], Lianfu Deng [b], Xiangyang Xu [b,*], Wenguo Cui [b,**], Hongyu Zhang [a,***]

[a] State Key Laboratory of Tribology, Department of Mechanical Engineering, Tsinghua University, Beijing, 100084, China
[b] Department of Orthopaedics, Shanghai Key Laboratory for Prevention and Treatment of Bone and Joint Diseases, Shanghai Institute of Traumatology and Orthopaedics, Ruijin Hospital, Shanghai Jiao Tong University School of Medicine, Shanghai, 200025, China
[c] Beijing Research Institute of Automation for Machinery Industry Co., Ltd, Beijing, 100120, China

ARTICLE INFO

Keywords:
Microfluidics
Hydrogel microspheres
Catecholamine chemistry
Hydration lubrication
Drug delivery

ABSTRACT

The occurrence of osteoarthritis (OA) is highly associated with the reduced lubrication property of the joint, where a progressive and irreversible damage of the articular cartilage and consecutive inflammatory response dominate the mechanism. In this study, bioinspired by the super-lubrication property of cartilage and catecholamine chemistry of mussel, we successfully developed injectable hydrogel microspheres with enhanced lubrication and controllable drug release for OA treatment. Particularly, the lubricating microspheres (GelMA@DMA-MPC) were fabricated by dip coating a self-adhesive polymer (DMA-MPC, synthesized by free radical copolymerization) on superficial surface of photo-crosslinked methacrylate gelatin hydrogel microspheres (GelMA, prepared via microfluidic technology), and encapsulated with an anti-inflammatory drug of diclofenac sodium (DS) to achieve the dual-functional performance. The tribological test and drug release test showed the enhanced lubrication and sustained drug release of the GelMA@DMA-MPC microspheres. In addition, the functionalized microspheres were intra-articularly injected into the rat knee joint with an OA model, and the biological tests including qRT-PCR, immunofluorescence staining assay, X-ray radiography and histological staining assay all revealed that the biocompatible microspheres provided significant therapeutic effect against the development of OA. In summary, the injectable hydrogel microspheres developed herein greatly improved lubrication and achieved sustained local drug release, therefore representing a facile and promising technique for the treatment of OA.

1. Introduction

One of the key pathogenies related with osteoarthritis (OA) is the greatly reduced lubrication, which can generally induce cartilage damage and a series of consecutive inflammation of the joint [1,2]. In most cases, artificial joint replacement would cause serious discomfort for the patient. As the recommended approach for the treatment of end stage OA in clinics, this surgery still remains multiple drawbacks, i.e. increased friction and wear of the artificial components [3]. Specific drugs taken via oral administration can alleviate the inflammation for early stage of OA [4], but it suffers from an extremely low absorption rate due to the deficiency of blood vessels in articular cartilage [5]. Alternatively, the local injection causes rapid drug failure with the risk of infection owing to frequent operations [6]. Consequently, developing an innovative non-surgical technique to achieve both improved lubrication and local drug delivery is greatly desirable in maintaining healthy joint, and it is also highly meaningful to reduce cartilage wear and relieve inflammatory symptom in OA treatment.

In recent years, injectable hydrogels have been developed with excellent biocompatibility and controlled drug delivery behaviors in

Peer review under responsibility of KeAi Communications Co., Ltd.
* Corresponding author.
** Corresponding author.
*** Corresponding author.
E-mail addresses: xu664531@163.com (X. Xu), wgcui80@hotmail.com (W. Cui), zhanghyu@tsinghua.edu.cn (H. Zhang).
[1] These authors contributed equally to this work.

https://doi.org/10.1016/j.bioactmat.2021.03.022
Received 17 December 2020; Received in revised form 10 March 2021; Accepted 11 March 2021

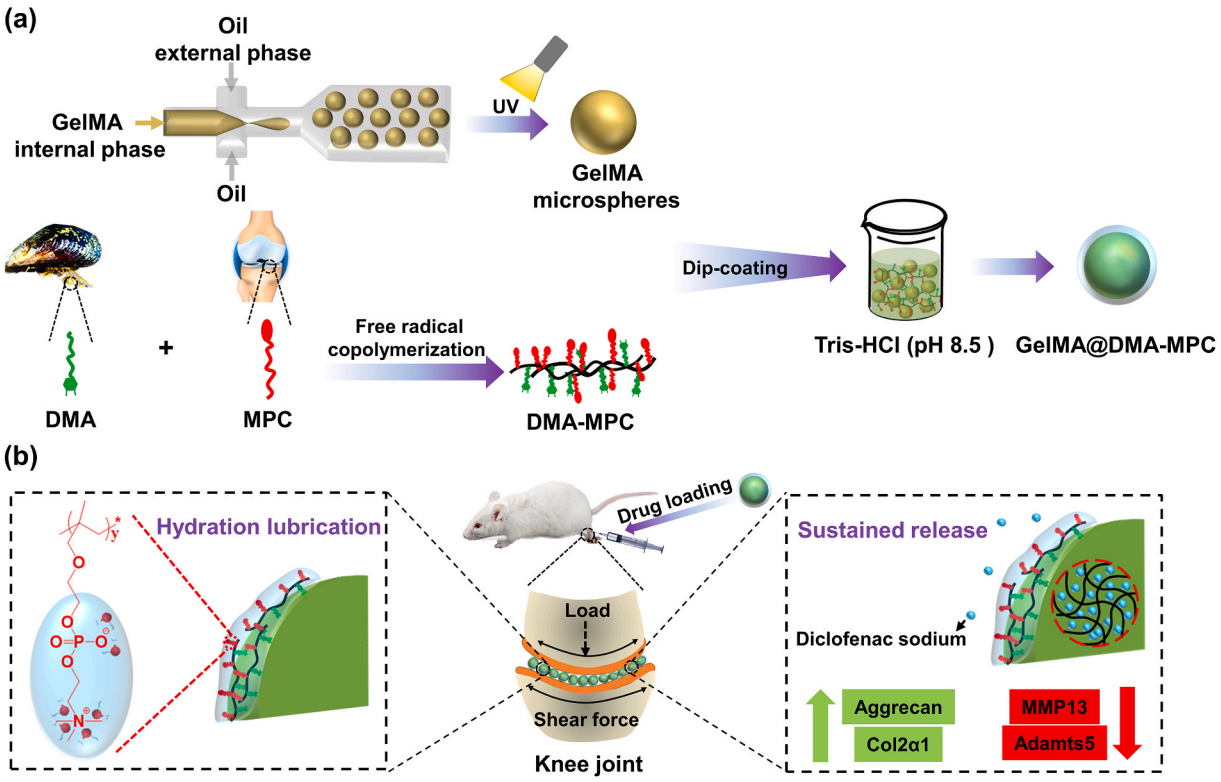

Fig. 1. Schematic illustration shows (a) the fabrication of GelMA microspheres by microfluidic technology, the synthesis of DMA-MPC polymer by free radical copolymerization, and the design of lubricated GelMA@DMA-MPC microspheres *via* the dip coating method; (b) the treatment of osteoarthritis by intra-articular injection of the drug-loaded and lubricated GelMA@DMA-MPC microspheres based on the synergistical intervention of enhanced lubrication and sustained drug release.

tissue engineering [7–9]. For example, Xin *et al.* [7] grafted protein on the surface of mesoporous bio-glass nanoparticles and photo-crosslinked together with methacrylate gelatin (GelMA) to prepare composite hydrogel, which could release the protein in a controllable program during the early bone regeneration period. However, two key drawbacks still remain. Firstly, a relatively high and uneven injection force is inevitable during the injection process owing to the non-uniform shape and large size of hydrogels [10], which may cause damage of the healthy tissue and discomfort of the patient. Secondly, limited lubrication enhancement has been considered for the hydrogels in the treatment of OA [11]. Unlike conventional hydrogels, the hydrogel microspheres possess significantly enhanced injectability due to the spherical shape and relatively uniform size [12]. Additionally, the flowability and flexibility of the microspheres allow them to disperse adequately in the solution and fulfill the requirement of joint loading. GelMA hydrogel microspheres prepared by microfluidic technology have been widely reported due to their enhanced structural stability, uniform size and high injectability [13]. However, previous studies have mainly focused on the property as drug delivery vehicles that aim to achieve sustained and controlled drug release in the joint [14]. For example, Chen *et al.* [15] encapsulated sinomenium into chitosan microspheres and photo-crosslinked GelMA hydrogel, and reported that the hydrogel could ameliorate osteoarthritis by regulating autophagy. Currently, the lubrication performance of injectable hydrogel microspheres has rarely been well studied, not to mention the discussion of the lubrication mechanism.

In a healthy joint, the synovial fluid consists of different biomacromolecules, which act as efficient lubricant participating in the boundary lubrication of the joint at physiological pressures [16,17]. The biomacromolecules are also the important constituents for articular cartilage. Recent studies have shown that the charged phosphatidylcholine lipids on the superficial surface of the articular cartilage contribute significantly to the reduced coefficient of friction (COF, 0.001–0.01). It is attributed to the hydration lubrication mechanism [18,19], in which the lipids can adsorb many water molecules to form a robust hydration layer surrounding the charges. The formation of the hydration layer is due to the charge-dipole interactions between the zwitterionic phosphocholine groups and the water molecules. Specifically, the hydration layer can rapidly relax when subjected to shear force, and thus induce a fluidlike response to decrease COF. In pathologies, the level of phosphatidylcholine lipids in the joint is reduced, and adequate bio-lubricants, as the precondition of proper joint movement, are crucial for preventing the development of degenerative changes in the joint [20]. Consequently, biomimetic poly (2-methacryloxyethyl phosphorylcholine) (PMPC), a typical derivative of the phosphatidylcholine lipids that can be grafted on the substrate, has been paid great attention as a lubrication material [21–23]. However, the severe reaction conditions and complicated synthesis steps limit its development and application in biomedical field.

Dopamine is a representative derivative of dihydroxy-phenylalanine that is contained in the adhesive proteins of mussel, and bioinspired dopamine-based multifunctional coatings have been greatly developed owing to the mild reaction conditions and self-adhesion properties [24–26]. In order to address the challenges as mentioned above, we innovatively propose a biomimetic strategy in the present study by synthesizing injectable hydrogel microspheres with enhanced lubrication and controllable drug release for the treatment of OA. As shown in Fig. 1, GelMA microspheres are prepared by microfluidic technology, and then dip coated by the biomimetic lubrication coating of DMA-MPC, which has been successfully developed in our previous studies [27–29], to generate the lubricating hydrogel microspheres (GelMA@DMA-MPC). Subsequently, the GelMA@DMA-MPC microspheres are loaded with an anti-inflammatory drug of diclofenac sodium (DS), and intra-articularly injected into the rat knee joint with an OA model to

examine the therapeutic effect. It is hypothesized that the GelMA@DMA-MPC microspheres developed herein may represent a facile and promising approach for preventing the development of degenerative changes in OA via the synergistical treatment of enhanced lubrication (COF reduction) and sustained drug release (inflammation down-regulation).

2. Materials and methods

2.1. Preparation of GelMA

GelMA was synthesized by gelatin (type A, Sigma-Aldrich, St. Louis, MO, USA) with the amidation reaction based on a previous study [30]. Briefly, gelatin (20 g) was first dissolved into Dulbecco's phosphate buffered saline (DPBS) (100 mL, Invitrogen, San Diego, CA) at 60 °C, and then methacrylic anhydride (16 mL, Aladdin Bio-Chem Technology Co., Ltd., Shanghai, China) was slowly added under continuous and vigorous stirring at 50 °C. The reaction was processed under N_2 atmosphere for 3 h. Afterwards, the mixture was diluted with fivefold DPBS at 40 °C to terminate the reaction. The solution was dialyzed against deionized water using 12000–14000 Da membrane, and purified at 40 °C for 7 d. Finally, the white porous foam product was obtained by freeze-drying and stored at −80 °C.

2.2. Preparation of microfluidic device

The microfluidic device was fabricated based on two kinds of syringe needles and plastic catheters [31]. Specifically, a tube-in-tube structure that contained both inner and external needles was manufactured by coaxially placing the two syringe needles, with the outer/inner diameters of 300/150 μm and 600/330 μm, respectively. All the connecting parts of the needles were tightly sealed by threaded caps and fixed with glue. Meanwhile, the microfluidic device was connected with the internal needle via a rubber hose (internal diameter: 1 mm), and the external needle was connected with a plastic catheter (internal diameter: 500 μm). Following extending the catheter by about 10 cm, a disc-like path (diameter: 10 cm) was shaped on a platform by hovering. Finally, an ultraviolet (UV) lamp was placed vertically above the platform at a distance of 8 cm, and the plastic catheter was extended by an extra length of 10 cm.

2.3. Microfluidic fabrication of GelMA microspheres

To fabricate GelMA hydrogel microspheres, the aqueous droplets within the internal aqueous phase were generated by the shear stress of continuous oil phase due to the flow-focusing geometry of the microfluidic device. Briefly, 5% (w/v) GelMA solution in phosphate buffer saline (PBS) supplemented with 0.5% photo-initiator 2-hydroxy-4'-(2-hydroxyethoxy)-2-methylpropiophenone (Irgacure 2959, PI, Sigma-Aldrich, St. Louis, MO, USA) served as the internal aqueous phase, i.e. the dispersed phase, while the continuous oil phase was composed of paraffin oil. 5% (w/w) Span 80 (Aladdin Bio-Chem Technology Co., Ltd., Shanghai, China) was used as the surfactant to stabilize the droplets.

The passage of internal hose was previously flushed with PBS. Afterwards, both phases were individually injected into the syringes, and the flow rates of liquid in different micro-channels of the syringe were adjusted by syringe pumps (LSP01-1A, LongerPump, China). After starting the pumps, the internal and continuous phases were slowly injected into the microfluidic device at the flow rates of 1.2 mL/h and 7.2 mL/h, respectively. The hydrogel droplets were further transported to the disc-like platform, and solidified by photo-crosslinking upon exposure to UV irradiation at the wavelength of 365 nm (6.9 mW/cm^2) for 20 s. Then, the photopolymerized microspheres were collected into each microtube, and washed repeatedly with acetone and 75% alcohol to remove the oil and surfactant, followed by washing with fresh PBS every 4 h for 24 h for further purification. Finally, the hydrogel microspheres were observed by a three-dimensional ultra-depth microscopy (VHX-5000, Keyence, China) and examined using a scanning electron microscope (SEM, SU8220, Hitachi, Japan) after freeze-drying.

2.4. Synthesis of DMA-MPC copolymer

Initially, DMA was synthesized according to our previous study [28]. Briefly, NaB_4O_7 (4 g) and sodium borate (10 g) were dissolved in deionized water (100 mL) under N_2 atmosphere, and dopamine hydrochloride (5 g, J&K Scientific Ltd., Beijing, China) was rapidly added. Meanwhile, methacrylic anhydride (5 mL) was mixed with tetrahydrofuran (25 mL), and then the mixture was added dropwise to the above dopamine solution. The pH value of the solution was adjusted to around 8 using sodium hydroxide and stirred for 12 h. Afterwards, hydrochloric acid was used to adjust the pH value of the reacted mixture to around 2. The solution was purged using acetic ether (60 mL) and magnesium sulfate. The product was precipitated by petroleum ether (500 mL) and collected by filtering. Finally, DMA was dried in vacuum to obtain the white solid power.

Subsequently, free radical polymerization was used to synthesize the DMA-MPC copolymer at three different mass ratios (1:4, 1:1 and 4:1). Briefly, DMA and MPC (Joy-Nature Institute of Technology, Nanjing, China) monomers were dissolved in N, N-dimethylformamide (40 mL) under N_2 atmosphere, and azodiisobutyronitrile (8 mg, Aladdin Bio-Chem Technology Co., Ltd., Shanghai, China) was rapidly added as the initiator. The mixture was stirred for 24 h at 70 °C to allow for reaction. Finally, the solution was dialyzed with deionized water for 3 d and freeze-dried for 1 week. ^{1}H-nuclear magnetic resonance (^{1}H NMR) spectrometer (JNM-ECS400, JEOL, Japan) was used to characterize the ^{1}H NMR spectrum of DMA and DMA-MPC copolymer, with dimethyl sulfoxide-d6 and D_2O (J&K Scientific Ltd., Beijing, China) as the deuterium solvent, respectively. The molecular weight (Mw) of the three kinds of copolymers were characterized by gel permeation chromatography (GPC, Viscotek TDA305max, Malvern Instruments, UK) using deionized water as the diluent at the flow rate of 0.7 mL/min.

2.5. Fabrication of DMA-MPC coated GelMA microspheres

The three mass ratios of the DMA-MPC copolymers (4 mg/mL) were dispersed in Tris-HCl buffer (pH = 8.5, 1 M) respectively, and then three equal volumes of microsphere solutions (2 mL) were added to the above solutions (4 mL), which were placed in a dark shaker for 24 h. Afterwards, the microspheres were collected by centrifugation and thoroughly rinsed with deionized water. The microspheres were freeze-dried and sputtered coated with platinum before investigation using the SEM in 5 kV. The surface elements of the samples were characterized by an X-ray photoelectron spectroscopy (XPS, PHI Quantera II, Ulvac-Phi Inc., Japan). The infrared spectra of the samples were recorded by a Fourier transform infrared spectrometer (FTIR, Bruker, Horiba, Germany).

2.6. Tribological test

The tribological tests were performed by a universal materials tester (UMT-3, Bruker Nano Inc., Germany) in a reciprocating mode at room temperature for 600 cycles. All the tribological experiments were completed with pin-on-disk friction pairs, using polytetrafluorethylene (PTFE) pin (diameter of contact surface: 5 mm) as the upper sample and silicon wafer as the lower sample. Specifically, 20 drops of different microspheres/PBS solutions (5 mg/mL) were dropped into the contact area as the lubricant before each experiment, with PBS as the control group. The oscillation amplitude was 4 mm, the sliding frequency was 1 Hz, and the normal load was 12 N. Each test was repeated at least three times to ensure data validity.

2.7. Drug loading and release

Firstly, 5 mg/mL of microspheres (uncoated and coated)/PBS solution (2 mL) was mixed with 2 mg/mL of diclofenac sodium/PBS solution (2 mL). To increase drug loading of the microspheres, dynamic adsorption was employed at a more violent shaking condition in a dark shaker for 24 h. Afterwards, the microspheres were collected by centrifugation and gently rinsed with PBS twice. The supernatant was mixed with the centrifugal solution to determine the drug loading by a UV–vis spectrophotometer (UV-8000, Metash Instruments, China). Subsequently, the drug-loaded microspheres were re-dispersed into 2 mL of fresh PBS before the release test in order to prevent the loss of drug during the transfer of the microspheres. Specifically, 2 mL of microspheres/PBS solution was encapsulated in 1 kD dialysis bag and immersed in 18 mL of PBS, which was then placed in the shaker for drug release at 37 °C and 60 rpm. At predetermined intervals, 2 mL of the medium outside the dialysis bag was removed, and the absorbance was recorded using the UV–vis spectrophotometer at the wavelength of 276 nm. 2 mL of fresh PBS was added to the solution after each measurement. The standard curve of diclofenac sodium in PBS was measured by the UV–vis spectrophotometer with the equation of $A = 34.77C + 0.0088$, where A is the absorbance of the solution, and C is the concentration of the solution. The drug loading efficiency (%) and the drug release percentage (%) were calculated based on the following equations.

$$Drug\ loading\ efficiency\ (\%) = \frac{Amount\ of\ loaded\ drug}{Total\ amount\ of\ drug\ (dosage)} \times 100\%$$

$$Drug\ release\ (\%) = \frac{Amount\ of\ released\ drug}{Total\ amount\ of\ loaded\ drug} \times 100\%$$

2.8. Degradation experiment

For the *in vitro* degradation experiment, GelMA and GelMA@DMA-MPC were immersed in 2 μg/mL of collagenase II/PBS solutions at 37 °C, and then placed in the shaker at 60 rpm. The two microspheres dispersed in PBS were set as the control groups. The collagenase II was used in the degradation experiment to mimic the physiological environment [30]. Periodically, the samples were examined by the three-dimensional ultra-depth microscope at 0, 2 and 4 weeks, respectively. Additionally, a quantitative evaluation of the degradation property of the hydrogel microspheres was performed. Briefly, GelMA and GelMA@DMA-MPC (1:1) (both were 10 mg) were dispersed in 2 μg/mL of collagenase II/PBS solutions (1 mL) at 37 °C, and then placed in the shaker at 60 rpm. At predetermined intervals, the supernatant of the collagenase solution was removed and the hydrogel microspheres were gently rinsed with deionized water twice. Subsequently, the samples were freeze-dried to obtain the remaining weight, and re-dispersed in fresh collagenase solution (1 mL). Each group was repeated for three parallel tests to ensure data validity. The degradation rate (%) of the microspheres was calculated based on the following equation.

$$Degradation\ rate\ (\%) = 1 - \frac{Remaining\ weight\ of\ microspheres}{Initial\ weight\ of\ microspheres} \times 100\%$$

2.9. Separation of rat chondrocytes

The rat chondrocytes were separated from articular cartilage according to our previous studies [32,33]. Briefly, the articular cartilage tissues were cut into small pieces, and then digested with 0.25% trypsin and 0.2% collagenase II for 30 min and 4 h, respectively. Afterwards, the isolated chondrocytes were cultured under 5% CO_2 atmosphere at 37 °C, using the Dulbecco's Modified Eagle's Medium/Nutrient Mixture F-12 (DMEM/F12, containing 1% antibiotics and 10% fetal bovine serum) as the medium. To maintain the chondrocytes phenotype, only the cells within the first three passages were utilized in the followed *in vitro* test.

2.10. Live/Dead staining assay

The cell viability of different GelMA microspheres was measured by Live/Dead cell staining kit (Life Tech, USA), in which the live cells were stained in green while the dead cells were stained in red under fluorescence microscope (ZEISS, Axio Imager M1, Germany). The chondrocytes with a density of 2×10^4 cells/mL were cultured in 24-well plates at 37 °C and 5% CO_2 atmosphere, and the culture medium was changed every two days. Subsequently, the chondrocytes were co-cultured with 1.5 mg/mL of GelMA, GelMA@DMA-MPC or GelMA@DMA-MPC@DS (0.25 mg/mL of DS)/PBS solutions for 1, 3 and 5 d in triplicate, using PBS as the blank group. Finally, the cells were stained with the Live/Dead cell staining dye (500 μL) for 15 min, and cell morphology was investigated by the fluorescence microscopy.

2.11. Cell cytotoxicity assay

The chondrocytes were cultured and co-cultured with the hydrogel microspheres similarly as before. The Cell Counting Kit-8 (CCK-8, Dojindo Kagaku, Japan) assay was used to evaluate cell cytotoxicity and cell proliferation at different time points (1, 3 and 5 d). Briefly, 50 μL of CCK-8 solution and 500 μL of fresh medium were added into each well, and the plates were incubated at 37 °C for another 2 h. Finally, the mixed solution was transferred to the 96-well plates in darkness, and the absorbance was measured through a microplate reader (Infinite F50, TECAN, Switzerland) at 450 nm.

2.12. Quantitative real-time polymerase chain reaction (qRT-PCR) analysis

The expression levels of inflammation-related factors in chondrocytes were recorded by the qRT-PCR via analyzing the transformation of OA-related genes. Similarly, the chondrocytes with a density of 2×10^5 cells/mL were cultured in the 6-well plates and treated with interleukin-1β (IL-1β, 5 nM) for 12 h to induce degeneration of the chondrocytes. Afterwards, the cells were co-cultured with 1.5 mg/mL of the above GelMA solutions for 24 h. The chondrocytes treated with IL-1β were nominated as the blank group, and the untreated chondrocytes were served as the control group. Subsequently, the total RNA of chondrocytes was extracted with TRIzol reagent (Invitrogen, USA) according to the previous study [34], and the purity and concentration of the RNA solutions were obtained by measuring the related absorbance at the wavelength at 280 nm and 260 nm. The corresponding cDNA was synthesized by 1 μg of RNA and a special Revert-Aid First Strand cDNA Synthesis Kit (TaKaRa, Dalian, China). The amplification process of cDNA mediated in qRT-PCR was completed with an ABI 7500 Sequencing Detection System (Applied Biosystems, Foster City, CA, USA) and a SYBR Premix Ex Tag Kit (TaKaRa, Dalian, China).

The relative mRNA expression levels of OA-related genes including aggrecan (Agg), collagen II (Col2α1), matrix metalloproteinase-13 (MMP13) and adamalysin-like metalloproteinases with thrombospondin motifs-5 (adamts5) were calculated by various specific primers, which were normalized to β-actin according to the $2^{-\Delta\Delta CT}$ method in a previous study [35]. The related primer sequences for the qRT-PCR test were listed as follows: β-actin: forward, 5'-CACTATCGGCAATGCGGTTCC-3'; reverse, 5'-CAGCACTGTGTTGGCATAGAGGTC-3'; Aggrecan: forward, 5′-GATCTCAGTGGGCAACCTTC-3'; reverse, 5′-TCCACAAACGTAATGCCAGA-3'; Col2α1: forward, 5′-CTCAAGTCG CTGAACAACCA-3'; reverse, 5′-GTCTCCGCTCTTCCACTCTG-3'; MM P13: forward, 5'-AACCAAGATGTGGAGTGCCTGATG-3'; reverse, 5'-CA CATCAGACCAGACCTTGAAGGC-3'; Adamts5: forward, 5′-TCCTCTT GGTGGCTGACTCTTCC-3'; reverse, 5′- TGGTTCTCGATGCTTGCAT GACTG-3'.

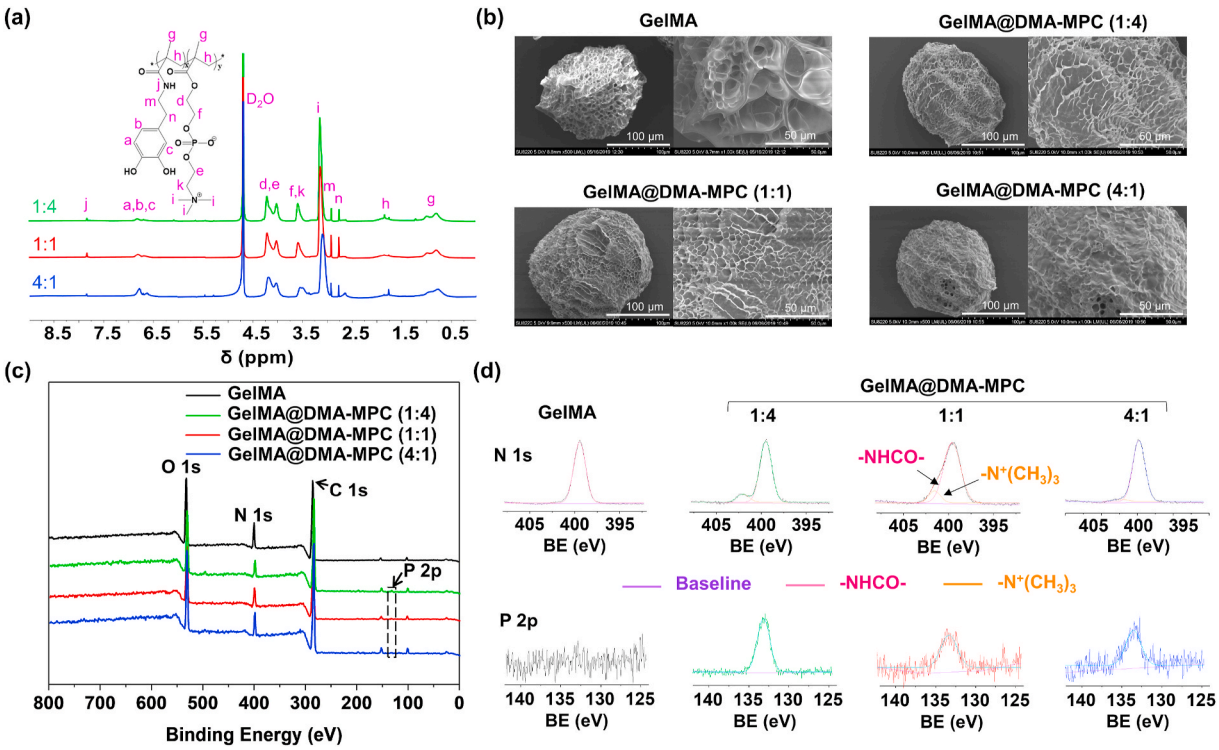

Fig. 2. Characterizations of the DMA-MPC copolymer and GelMA microspheres. (a) ^{1}H NMR spectra of the DMA-MPC copolymers with three different mass ratios. (b) SEM morphologies of the GelMA and GelMA@DMA-MPC microspheres after freeze-drying. (c) XPS spectra and (d) the deconvolution analysis of N 1s and P 2p of the GelMA and GelMA@DMA-MPC microspheres. BE: binding energy.

2.13. Immunofluorescence staining assay

The chondrocytes with a density of 1×10^4 cells/mL were cultured in the 24-well plates with sterile cover glasses, treated with IL-1β (5 nM) for 12 h, and then co-cultured with 1.5 mg/mL of the above GelMA solutions. After co-culturing for 12 h, the chondrocytes were fixed with 4% paraformaldehyde for 10 min, and then permeabilized with 0.1% Triton X-100 (Aladdin Bio-Chem Technology Co., Ltd., Shanghai, China) and blocked with 3% bovine serum albumin/phosphate buffered saline (BSA/PBS, Aladdin Bio-Chem Technology Co., Ltd., Shanghai, China) at 25 °C for 15 min and 30 min, respectively. After washing with PBS, the cells were stained against the specific rat primary antibody of anti-Col2α1 (at 1:200 dilution, Abcam, USA) overnight at 4 °C. Subsequently, the cells were gently washed with PBS and reacted against the specific Alexa Fluor-coupled secondary antibodies (1:400 dilution, Molecular Probes, Life Tech, USA) at 25 °C for 1 h in darkness. Meanwhile, the cell nuclei were counterstained using 4, 6-diamidino-2-phenyindole dilactate (DAPI, Life Tech, USA) in darkness for 15 min, and the cell actin was labeled by Alexa Fluor 594 phalloidin (Life Tech, USA). Finally, the staining images were captured using a laser scanning confocal microscope (LSM800, ZEISS, Germany), and the expression of Col2α1 was investigated by the Image J software.

2.14. Rat osteoarthritis model and surgical process

All the animal experiments involved were authorized by the Animal Research Committee of Ruijin Hospital, School of Medicine, Shanghai Jiaotong University, China, and all the surgical operations were approved by the National Institutes of Health Guidelines for the Care and Use of Laboratory Animals. The rat osteoarthritis model was designed by destabilization of the medial meniscus (DMM) surgery in twenty-five male Sprague-Dawley rats (12 weeks old and 200–250 g weight). Firstly, the rats received intraperitoneal anesthesia via injection of pentobarbital sodium (30 mg/kg weight). After sterilization, the knee joint of right limb was exposed, and a medical lateral incision was arranged. Skin incision was performed from the distal patella to proximal tibial plateau. Subsequently, the patellar tendon in knee joint capsule was spread open with scissors. The patellar tendon was retracted, and the medial meniscus ligament (MMTL) was exposed through the blunt dissection of fat pad. After that, the MMTL was sliced with a microsurgical knife, and the wound incision was well sutured. Additionally, a sham operation was performed by the same method without the MMTL transection. The rats were provided with sufficient food and water and allowed to move without any restriction. One week later, the rats were randomly divided into five groups (five rats for each group), and four groups of them were intra-articularly injected with 50 μL of PBS, GelMA, GelMA@DMA-MPC or GelMA@DMA-MPC@DS (1.5 mg/mL in PBS), respectively. The injection was performed once every two weeks for a total duration of 8 weeks. Additionally, all the rats obtained the special running exercise for 1 h at a speed of 20 m/min every two days on a level treadmill in order to accelerate the induction of osteoarthritis at the knee joint.

2.15. X-ray radiography and histological staining

All the rats were scanned using an X-ray imager (Faxitron X-ray, USA) after surgery at 1 and 8 weeks, with 32 kV voltage and 6 mA s exposure time, and the articular space width of the knee joint was measured based on the X-ray radiographs. Afterwards, the rats were sacrificed, and the knee joints were fixed in 4% paraformaldehyde for 24 h and subsequently decalcified in the 10% ethylene diamine tetraacetic acid (EDTA). Meanwhile, the vernier caliper was utilized to measure the macroscopic cartilage lesion depth. All the samples were dehydrated in ethanol and pruned in half, and the medial condyle was embedded within paraffin (Yihui Bio Tech., Co., Ltd., Shanghai, China). Subsequently, the continuous paraffin sections were prepared (thickness: 5 μm) and stained alternately with H&E and safranin O-fast green. Moreover, the sections with safranin O-fast green were investigated

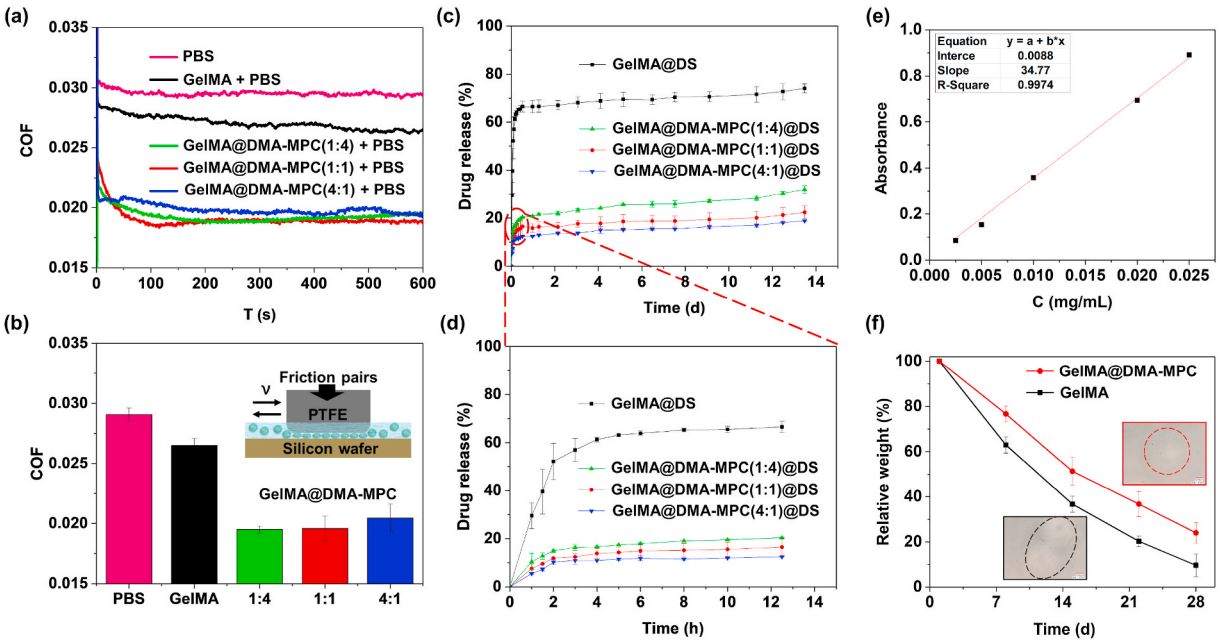

Fig. 3. The lubrication, drug release and degradation properties of GelMA and GelMA@DMA-MPC microspheres. Tribological tests are performed by UMT-3 with a typical friction pair using PTFE pin and silicon wafer. (a) COF–time plots and (b) COF histograms for PBS, GelMA and the three kinds of GelMA@DMA-MPC microspheres in PBS (5 mg/mL) under the loading of 12 N. Drug release profiles of the GelMA and GelMA@DMA-MPC microspheres in PBS (37 °C) for (c) 14 d and (d) the first 13 h. (e) The standard curve of DS in PBS. (f) The quantitative degradation curve of GelMA and GelMA@DMA-MPC (1:1) in PBS with 2 μg/mL of collagenase II. The two illustrations are the microscope images of the microspheres after degradation for 28 d.

based on the Osteoarthritis Research Society International (OARSI) standard [36], which could score the materials in four stages (degree of involvement) and six grades (depth of lesion) in the range from 0 (normal) to 24 (severe osteoarthritis). Finally, the related relative glycosaminoglycan (GAG) contents were assessed by the Image J software based on the safranin O-fast green staining.

2.16. Statistical analysis

The data were shown as mean ± standard deviation (SD). Each independent test was repeated at least three times with parallel tests to ensure validity. Statistical analysis was performed using the GraphPad Prism software (Version 5.0, GraphPad Software Inc., USA). One-way analysis of variance (ANOVA) was carried out for the multiple comparison tests, and two-tailed non-paired Student's t-test was performed for the two comparison tests. The statistical significance was set as $^{*}P < 0.05$ and $^{\#}P < 0.05$.

3. Results and discussion

3.1. Characterization of GelMA and DMA-MPC coated GelMA microspheres

The GelMA hydrogel microspheres were fabricated by photopolymerization of the GelMA droplets based on microfluidic technology. Meanwhile, self-anchoring agent DMA monomer and DMA-MPC copolymer were synthesized by amidation reaction and free radical copolymerization, respectively. To study the lubrication property of diverse content of MPC groups, we synthesized DMA-MPC with three mass ratios (1:4, 1:1 and 4:1), which were coated on the surface of GelMA microspheres for screening, namely GelMA@DMA-MPC. Fig. 2a displays the ^{1}H NMR spectra of the three kinds of DMA-MPC. The signals at 7.82 and 6.85–6.71 ppm are assigned to –NHCO– and trihydrophenyl groups of DMA, and the signal at 3.18 ppm is attributed to the special groups of MPC. This result proves that the DMA-MPC copolymer has been successfully synthesized. The presence of catechol groups (phenolic hydroxyl groups) in the DMA-MPC copolymer indicates that it maintains the adhesive property similar to dopamine. The catechol groups are susceptible to oxidation to quinone under neutral or alkaline conditions, and strong chemical bonds are formed between the copolymer and the active hydrogen of hydroxyl on the substrate [24]. Additionally, the GPC result in Fig. S1 shows that the Mw of the DMA-MPC (1:4), DMA-MPC (1:1) and DMA-MPC (4:1) copolymers are 3.78E6, 2.27E6 and 1.64E6 Daltons, with the polydispersity of 5.9, 5.3 and 4.1, respectively. This result further indicates that the polymerization reaction has been successful.

The SEM images in Fig. 2b illustrate the morphologies of GelMA and GelMA@DMA-MPC after freeze-drying. Clearly, the surfaces of the functionalized microspheres are covered with copolymers by varying degrees, and some of the pores in the microspheres have disappeared. The GelMA@DMA-MPC microspheres with the mass ratio of 4:1 are coated with more copolymers due to the higher proportion of the anchoring agent. The GelMA microspheres have a mean size of approximately 150 μm, showing porous structure with different pore sizes due to the crosslinked mesh structure of GelMA. The GelMA microspheres without freeze-drying demonstrate smooth morphology, which are observed by the microscopy (Fig. S2). The characteristic element P 2p (133.3 eV) in XPS indicates the successful surface modification of the copolymers on the GelMA microspheres (Fig. 2c), and it is further confirmed by the narrow spectrum of P element in the high-resolution XPS as shown in Fig. 2d. Additionally, the transformation ratio of element N 1s (402.0 eV) also proves the presence of the coatings on the surface of the microspheres. N element in the narrow spectrum is deconvoluted into two types for GelMA@DMA-MPC including both amide group (–NHCO–) and quaternary ammonium group ($–N^{+}(CH_3)_3$), while only amide group (–NHCO–) is observed for GelMA. Moreover, the absorption peaks of the phosphate stretching vibration and benzene skeleton vibration in the Fourier transform infrared spectra further verify the modification of the copolymers on the GelMA microspheres, as shown in Fig. S3. Overall, the above material characterizations support the successful preparation of the copolymers and the copolymers-coated GelMA microspheres.

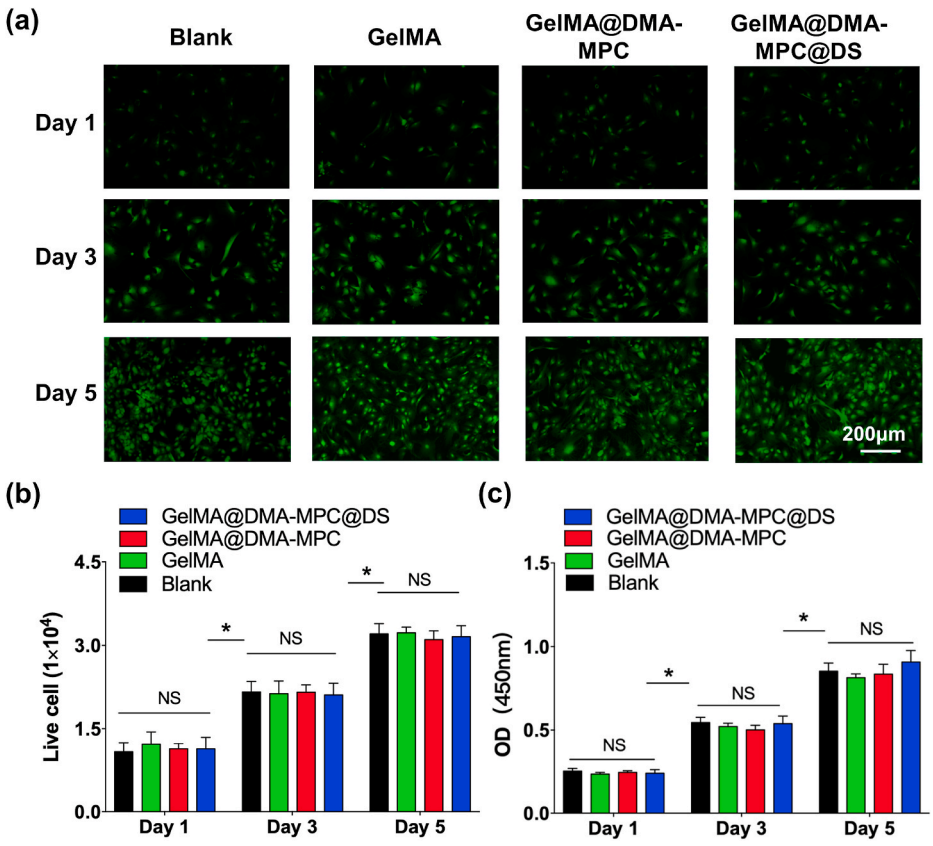

Fig. 4. *In vitro* cell viability and cell cytotoxicity of three different GelMA microspheres. (a) Representative fluorescence images observed by Live/Dead staining assay shows the viability of chondrocytes co-cultured with the GelMA, GelMA@DMA-MPC and GelMA@DMA-MPC@DS microspheres for 1, 3 and 5 d. (b) Quantitative evaluation of live cells from Live/Dead staining assay. (c) CCK-8 assay demonstrates the cytotoxicity of three different GelMA microspheres in cell proliferation. (n = 3, NS: no significance, * represents $P < 0.05$ by comparing with the blank group).

3.2. Lubrication performance

A series of tribological tests were performed employing the UMT-3 in reciprocating mode to investigate the lubrication property of GelMA and GelMA@DMA-MPC, using a typical friction pair with PTFE pin and silicon wafer [37,38]. The COF–time plots and COF histograms are shown in Fig. 3a–b. It is clear that the COF of GelMA with or without DMA-MPC is lower compared with PBS. Particularly, GelMA@DMA-MPC at the mass ratio of 1:4 has the most significant reduction in COF, where the COF value decreases dramatically from 0.027 to 0.019 (~29.6%). The GelMA microspheres themselves contribute to bearing capacity and lubrication ability due to the efficient elastic and rolling properties. Besides, the lubrication performance of GelMA@DMA-MPC is better than GelMA, which further reduces COF synergistically via hydration lubrication of the zwitterionic phosphocholine groups in the copolymers [19]. Additionally, it is speculated that the DMA-MPC coating layer may also behave as a "lubricant" between the microspheres, and consequently it avoids jamming of the microspheres in the rolling process, which is favorable for lubrication [39,40].

3.3. Drug release property

DS is a common nonsteroidal anti-inflammatory drug and has been used for the treatment of OA [4]. As an effective carrier, GelMA microspheres can not only prevent the rapid loss of drug, but also achieve sustained local drug release. The standard curve of DS in PBS is depicted in Fig. 3e. The drug loading efficiency of the hydrogel microspheres (bare GelMA and the three kinds of functionalized GelMA) is 10.4%, 16.1%, 10.5% and 15.5%, respectively. The controlled drug release property of GelMA@DS and GelMA@DMA-MPC@DS is determined by measuring the absorbance value of DS with the UV–vis spectrophotometer. Fig. 3c–d shows the result of drug release behavior of the microspheres at each time point. Obviously, the drug release of the three GelMA@DMA-MPC@DS is significantly lower than that of GelMA@DS, in both the initial burst release stage and the relative plateau stage afterwards. For example, the drug release reduces from approximately 66% to the range from 12 to 20% in the first 2 days after coating with DMA-MPC, which indicates that the copolymer can effectively control burst drug release and achieve sustained drug release. GelMA@DMA-MPC@DS with the mass ratio of 4:1 is relatively more effective in the control of drug release due to the relative denser coating on the surface of the microspheres. However, there is no obvious difference among the GelMA@DMA-MPC@DS with different mass ratios in the drug release rate. Therefore, synergistically considering the properties of lubrication enhancement and drug release, GelMA@DMA-MPC@DS with the mass ratio of 1:1 is selected as the microspheres for the subsequent experiments.

3.4. Degradation property

The degradation property of the intra-articularly injected biomaterials is important for the treatment of OA. Fig. S4 shows the degradation performance of GelMA and GelMA@DMA-MPC (1:1) with or without collagenase II (2 μg/mL) in PBS. Upon 4 weeks of incubation, all the microspheres without collagenase II have excellent stability, with only slight hydrolysis, while the microspheres exhibit sequential biodegradability in the presence of collagenase II. Practically, the microspheres degrade gradually in a surface corrosion degradation mode from outside to inside, and small particles formed due to surface degradation are detected from the images with higher magnification, as shown in Fig. 3f. Moreover, the results of degraded microscope images are consistent with the quantitative performance obtained by weight change. The degradation rate of GelMA@DMA-MPC is lower than that of GelMA (76.0% and 90.3% at 28 d), although they both degrade gradually over time in collagenase solutions. Generally, the bioinspired lubrication coating can effectively reduce the degradation performance

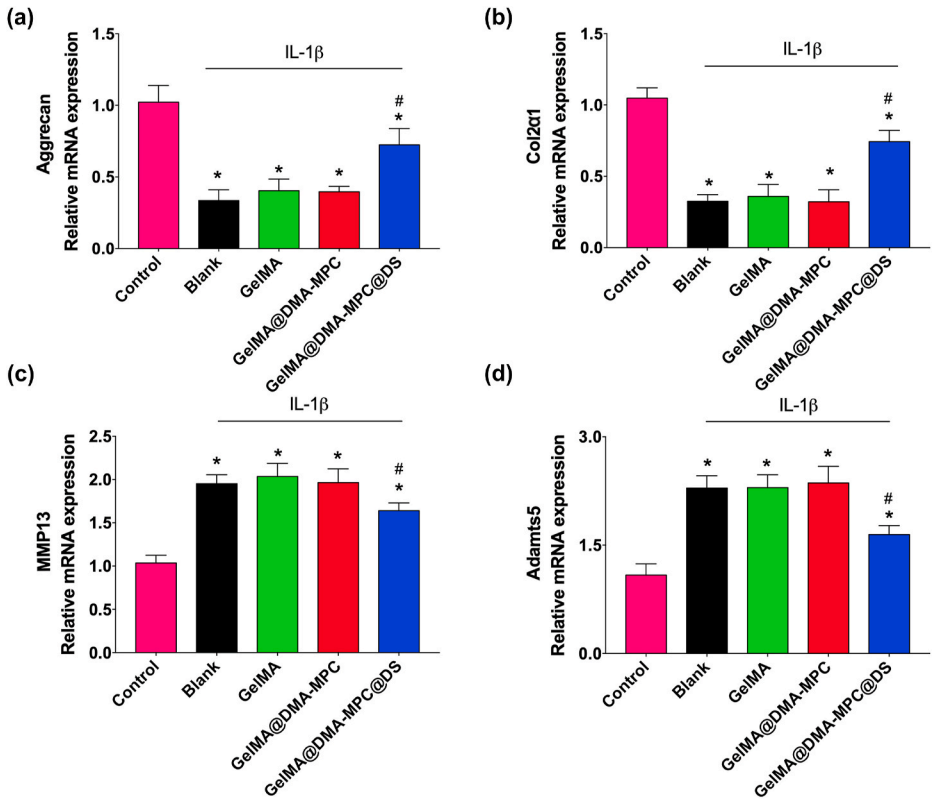

Fig. 5. qRT-PCR analysis shows the mRNA expression levels of (a) aggrecan, (b) Col2α1, (c) MMP13 and (d) adamts5 in the IL-1β treated chondrocytes, which are co-cultured with the GelMA, GelMA@DMA-MPC and GelMA@DMA-MPC@DS hydrogel microspheres for 24 h (n = 3, * and # represent $P < 0.05$ by comparing with the control and blank groups, respectively).

of the hydrogel microspheres, which may be attributed to the physical barrier of the hydration layer surrounding the zwitterionic headgroups in the copolymer. Overall, the optimal lubrication biomaterials should be weakly biodegradable, and the qualitative and quantitative results of the hydrogel microspheres indicate that GelMA@DMA-MPC is more stable than GelMA due to the presence of the DMA-MPC coating on the surface, which is desirable for intra-articular treatment of osteoarthritis.

3.5. Cell viability and cell cytotoxicity in vitro

It is essential to investigate cell cytotoxicity and the protective effect of inflammation-induced chondrocytes degeneration *in vitro* in order to determine the feasibility of using GelMA@DMA-MPC@DS for OA therapy. We first characterized cytocompatibility of different GelMA hydrogel microspheres by Live/Dead cell staining and CCK-8 assay. As shown in Fig. 4a, the viability of chondrocytes co-cultured with GelMA, GelMA@DMA-MPC and GelMA@DMA-MPC@DS for 1, 3, and 5 d is examined by Live/Dead staining assay. Clearly, dead cells (red staining) are hardly observed in all the groups, and live cells (green staining) exhibit favorable viability at the time points. It is noteworthy that the cell density gradually increases with cultured time, which is further confirmed by the quantitative evaluation of live cells in Fig. 4b. The number of live cells in the experimental groups is almost the same as the blank (PBS) group, indicating that the microspheres have no detrimental effect on the cells. Furthermore, the CCK-8 assay in Fig. 4c indicates that there is no significant difference in cell proliferation among the three groups. All these cellular findings together prove that the GelMA microspheres exhibit excellent biocompatibility and no cytotoxicity to the chondrocytes, which is a prerequisite for the *in vivo* experiments and clinical applications.

3.6. Protective effect on inflammation-induced chondrocytes degeneration

Chondrocytes degradation is a typical feature of OA, in which inflammatory mediation acts as an important factor in activation of pathogenesis [32]. To examine the protective effect of the microspheres for inflammation-induced chondrocytes degeneration *in vitro*, the expression levels of four kinds of OA-related genes are recorded by qRT-PCR. Particularly, the selected OA-related genes include (a) Agg and Col2α1, which are the important constituents of extracellular matrix due to their necessity for cartilage regeneration, and (b) MMP13 and adamts5, which are typically involved in cartilage degeneration and metastasis. The up-regulation of MMP13 and adamts5 results in progressive cartilage degeneration. To form an inflammatory environment, in this study we introduced a pro-inflammatory cytokine lymphocyte stimulating factor (IL-1β) to induce chondrocytes degradation, and co-cultured the chondrocytes with the GelMA microspheres for 24 h. The expression levels of each gene were analyzed to evaluate the protective effect of the microspheres for cartilage degradation.

As can be seen in Fig. 5a–b, a significant reduction in the relative mRNA expression levels of Agg and Col2α1 is observed after IL-1β treatment (nominated as blank group), compared with the untreated group (control group). The GelMA@DMA-MPC@DS group exhibits a significant increase in the relative gene expression levels compared with the blank group, but there is limited effect for the GelMA and GelMA@DMA-MPC groups. The result indicates that GelMA@DMA-MPC@DS can promote the expression of anabolic factors (Agg and Col2α1) and thus protect the chondrocytes to some extent. On the other hand, the anti-inflammatory effects of the microspheres are further assessed by the expression of degradation factors including MMP13 and adamts5. The blank group treated with IL-1β has higher mRNA expression levels of MMP13 and adamts5 compared with the untreated group, as shown in Fig. 5c–d. There is no significant change for the GelMA and

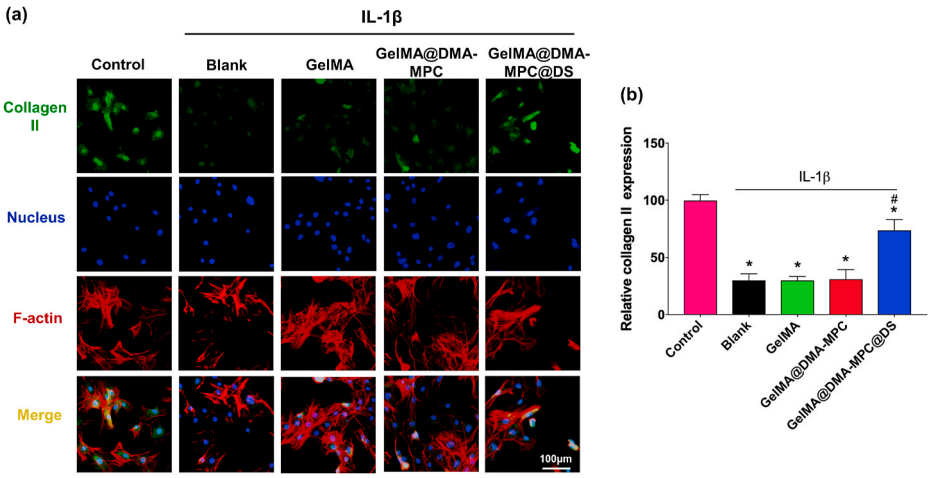

Fig. 6. (a) Representative immunofluorescence staining images display the protein expression level of collagen II in the IL-1β treated chondrocytes, which are co-cultured with the GelMA, GelMA@DMA-MPC and GelMA@DMA-MPC@DS hydrogel microspheres for 12 h. Green: collagen II; Blue: cell nuclei; Red: cell F-actin. (b) The quantitative data show the comparison of protein expression level of collagen II via fluorescence intensity. (n = 3, * and # represent P < 0.05 by comparing with the control and blank groups, respectively).

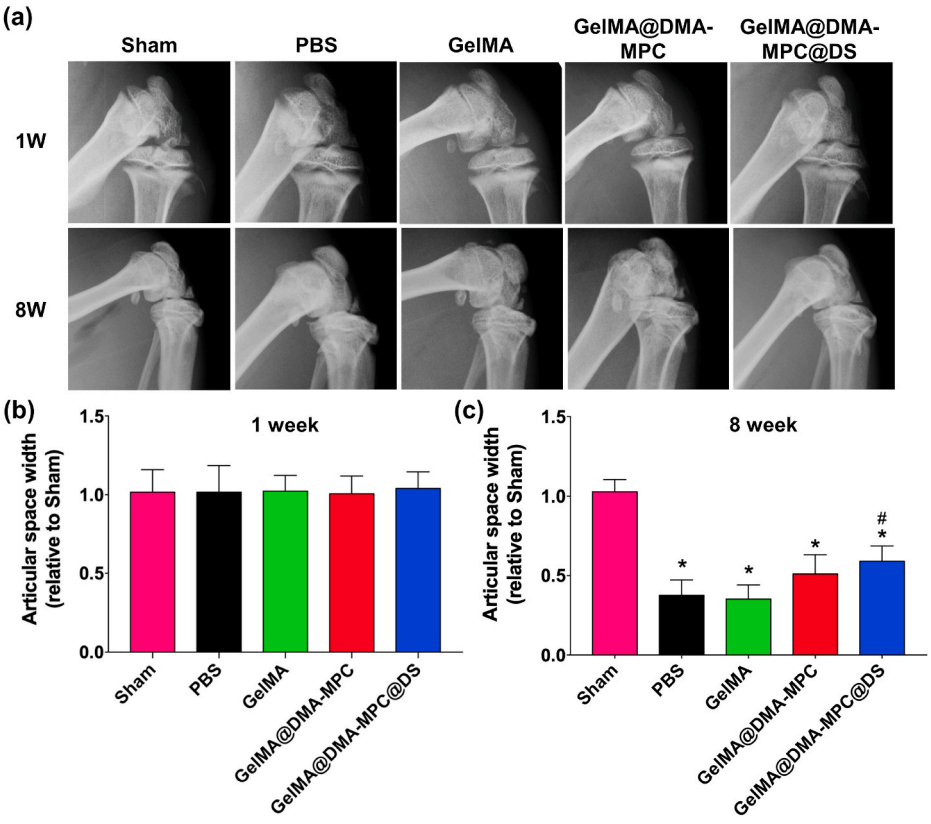

Fig. 7. The functionalized GelMA microspheres reduce the joint space narrowing *in vivo*. (a) Representative X-ray radiographs of knee joint for five groups of rats at 1 and 8 weeks after the DMM surgery, which receive intra-articular injection of PBS, GelMA, GelMA@DMA-MPC and GelMA@DMA-MPC@DS for the treatment of osteoarthritis. The relative articular space width of different groups at (b) 1 week and (c) 8 weeks after the DMM surgery, which is determined from the X-ray radiographs. (n = 5, * and # represent P < 0.05 by comparing with the sham and PBS groups, respectively).

GelMA@DMA-MPC groups in comparison with the blank group. In contrast, the IL-1β treated chondrocytes that are co-cultured with GelMA@DMA-MPC@DS show remarkable down-regulation of MMP13 and adamts5, which clearly indicates the anti-inflammatory effect of GelMA@DMA-MPC@DS for chondrocytes degeneration. Overall, the results of up-regulation of anabolic factors (Agg and Col2α1) and down-regulation of pro-inflammatory factors (MMP13 and adamts5) demonstrate that GelMA@DMA-MPC@DS possesses the desirable chondroprotective potential for inflammation-induced chondrocytes degeneration. However, it should be noted that no significant improvement is observed for the GelMA@DMA-MPC group in regulating the gene expressions compared with the blank group, because no lubrication effect is involved in the current *in vitro* evaluation.

Furthermore, the chondrocytes were treated for immunofluorescence staining assay to verify the regulation effect of the hydrogel microspheres on the inflammatory factors. The representative fluorescence images in Fig. 6a visually display the protein expression of Col2α1 in chondrocytes via fluorescence intensity. After treatment with IL-1β, a significant reduction is observed in the blank group, and there is no significant difference in the GelMA and GelMA@DMA-MPC groups. However, the GelMA@DMA-MPC@DS group remarkably increases the expression of Col2α1 at the protein level. Moreover, the corresponding statistical analysis in Fig. 6b quantitatively shows the effect with the increase of anabolic protein expression in the inflammatory chondrocytes, which is consistent with the qRT-PCR characterization as mentioned above. These results further support that GelMA@DMA-MPC@DS is the most effective biomaterial to protect the chondrocytes from inflammation-induced degeneration.

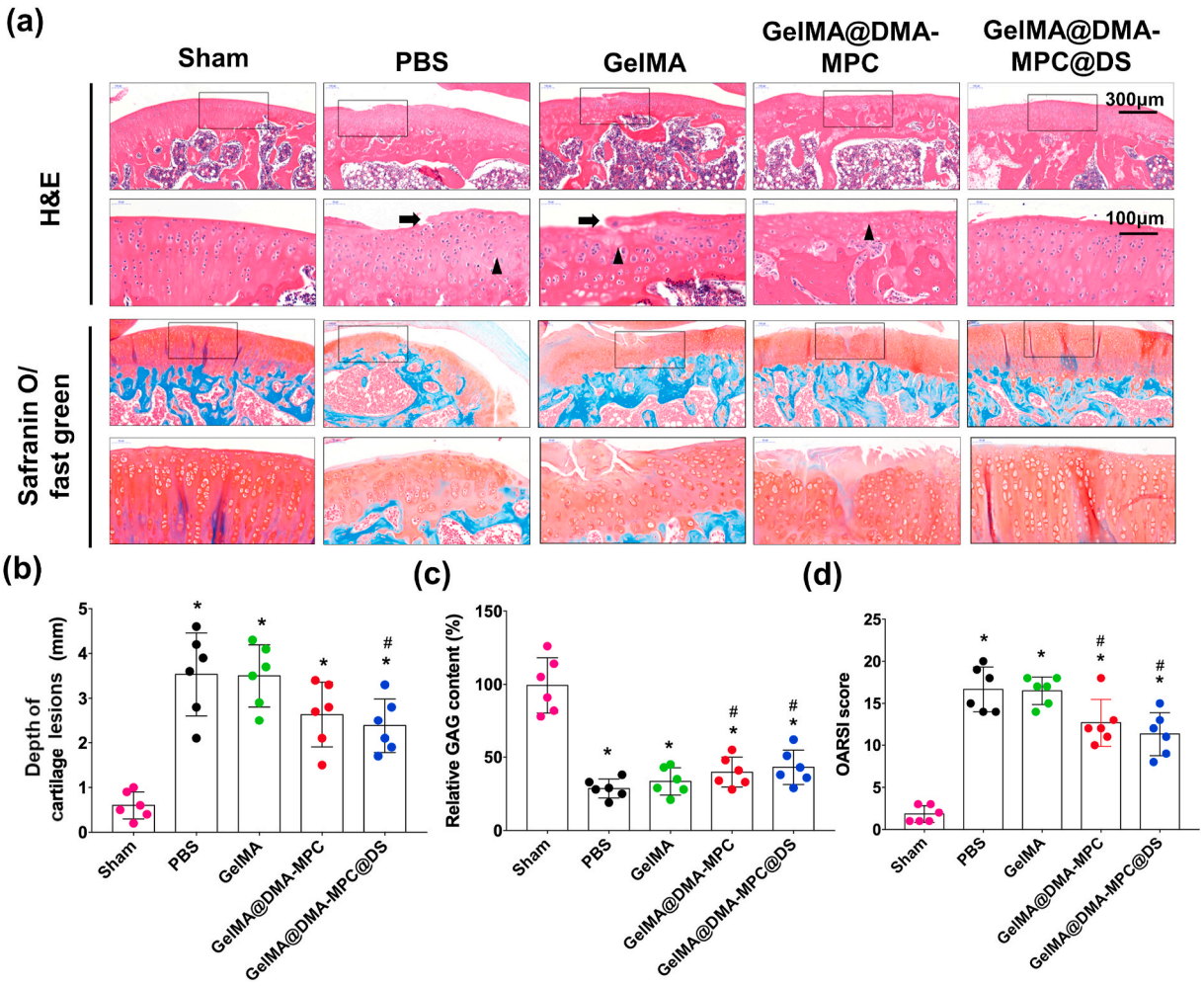

Fig. 8. The functionalized GelMA microspheres delay the progression of osteoarthritis *in vivo*. (a) Representative images of H&E staining and Safranin O-fast green staining in the histological staining assay display the histological changes in various degrees of cartilage section for different groups of rats at 8 weeks after the DMM surgery. The black arrow shows erosion fissures, and the black triangle represents tissue cellularity with cloning. (b) The corresponding depth of cartilage lesions, (c) relative GAG content and (d) OARSI score of articular cartilage in different groups of rats. (n = 5, * and # represent $P < 0.05$ by comparing with the sham and PBS groups, respectively).

3.7. Therapeutic effect of osteoarthritis in vivo

To characterize the therapeutic effect of GelMA@DMA-MPC@DS on OA *in vivo*, the rat OA model was first established by DMM surgery according to a previous study [33]. One week later, different groups of rats were intra-articularly injected with PBS, GelMA, GelMA@DMA-MPC or GelMA@DMA-MPC@DS once every two weeks for a total of 8 weeks, respectively. X-ray radiograph and histological staining assay were performed to evaluate the therapeutic effect on OA. All the rats survived well and no infection was observed during the whole experiment.

Fig. 7a shows the representative X-ray radiographs of the rat knee joints at 1 and 8 weeks after the DMM surgery. It is clear that the morphologies of all rat knee joints are normal at 1 week after the surgery, and it is similar in the articular space width among different groups, which is also illustrated by the histogram (relative to sham group) in Fig. 7b. The articular space widths of the four experimental groups become narrower at 8 weeks after the surgery, while it remains relatively unchanged in the sham group. This result indicates the successful establishment of the OA model by the DMM surgery. Importantly, the articular space width of the GelMA@DMA-MPC group is much higher than that of the GelMA group, although there is no significant difference between the GelMA group and the PBS group. The result indicates that the involvement of the copolymer with lubrication property is beneficial to inhibit the development of OA. Moreover, a relatively larger articular space width is observed for the GelMA@DMA-MPC@DS group compared with that of the GelMA@DMA-MPC group (Fig. 7c), which indicates that GelMA@DMA-MPC@DS has a better inhibition effect of OA owing to the synergetic contribution of enhanced lubrication and sustained drug release.

To further determine whether the hydrogel microspheres would delay the progression of OA, the cartilage tissues were performed with histological staining assay including hematoxylin-eosin (H&E) staining and safranin O-fast green staining. As shown in Fig. 8a, it's clear that the PBS group presents typical features of osteoarthritis such as surface discontinuity, erosion fissures and deformation. The GelMA group displays no significant difference compared with the PBS group. However, in comparison with the GelMA group, the GelMA@DMA-MPC and GelMA@DMA-MPC@DS groups demonstrate significant improvement in morphology change, tidemark integrity, matrix staining and tissue cellularity with cloning in varied degrees. Similarly, the GelMA@DMA-MPC@DS group is also considered as the most effective material in safranin O-fast green staining due to the most intense positive staining. Importantly, it is noted that the depth of cartilage lesions (Fig. 8b) of the GelMA@DMA-MPC and GelMA@DMA-MPC@DS groups decrease greatly compared with the PBS group (24.1% and 34.9%, respectively), which indicates that intra-articular injection of functionalized

microspheres can effectively prevent the deterioration of cartilage tear. Although there is a significant reduction for the four experimental groups in comparison with the sham group, the GAG contents of the three microspheres groups all increase compared with the PBS group. The GelMA@DMA-MPC@DS group exhibits the best result in GAG content among the four experimental groups, with 50.5% increase relative to the PBS group as shown in Fig. 8c. The finding suggests that GelMA@DMA-MPC@DS protects articular cartilage via promoting GAG deposition and maintaining cartilage thickness. Additionally, the GelMA@DMA-MPC@DS group also has the lowest value of OARSI score among the four experimental groups (Fig. 8d). In summary, the progression of OA has been inhibited at the greatest level in the GelMA@DMA-MPC@DS group, as evidenced by the significant improvement in GAG deposition and cartilage morphology, and also by the reduction of the depth of cartilage lesions, OARSI score and cartilage matrix depletion. The results together indicate that the functionalized hydrogel microspheres have the most promising therapeutic effect for the treatment of OA based on the synergistical effect of enhanced lubrication and sustained drug release. Additionally, it is shown in our previous study that DMA (contained in DMA-MPC) has potential anti-inflammatory property, which can act as reactive oxygen species (ROS) scavenger to efficiently eliminate the ROS radicals [41]. The effect is attributed to the antioxidant function of the hydroquinone moiety in DMA, and it may contribute to the treatment of OA for the functionalized hydrogel microspheres.

4. Conclusions

In the present study, inspired by the properties of self-adhesive mussel and super-lubricating cartilage, we innovatively designed and synthesized injectable GelMA@DMA-MPC microspheres with a combination of biomimetic lubrication coating and drug delivery vehicle. The lubricated microspheres were encapsulated with DS for the treatment of OA. The GelMA@DMA-MPC@DS could protect articular cartilage and alleviate inflammation owing to the enhanced lubrication and sustained drug release, which were proved by the lubrication and drug release tests. Additionally, the *in vitro* cell tests demonstrated that the biocompatible microspheres significantly upregulated the expression levels of cartilage anabolic genes and simultaneously downregulated the expression levels of cartilage catabolic proteases genes. Furthermore, the *in vivo* experiments revealed that all the indicators of the GelMA@DMA-MPC@DS group were at the highest level in OA treatment, which indicated that the functionalized microspheres provided positive therapeutic effect against the development of OA. In conclusion, the functionalized microspheres developed herein have the potential to be a promising method for inhibiting the degenerative changes in early OA, yet further animal and ultimately human studies are necessary before the microspheres are authentically used for the treatment of OA in clinics.

CRediT authorship contribution statement

Ying Han: Investigation, Methodology, Writing – original draft. **Jielai Yang:** Investigation, Methodology. **Weiwei Zhao:** Methodology, Formal analysis. **Haimang Wang:** Formal analysis. **Yulong Sun:** Formal analysis. **Yuji Chen:** Methodology. **Jing Luo:** Visualization. **Lianfu Deng:** Resources. **Xiangyang Xu:** Conceptualization, Resources. **Wenguo Cui:** Conceptualization, Resources, Funding acquisition. **Hongyu Zhang:** Conceptualization, Resources, Writing – review & editing, Funding acquisition.

Declaration of competing interest

The authors declare that they have no competing interests.

Acknowledgements

This study was financially supported by National Natural Science Foundation of China (52022043 and 81930051), Tsinghua University-Peking Union Medical College Hospital Initiative Scientific Research Program (20191080593), Precision Medicine Foundation, Tsinghua University, China (10001020107), Shanghai Jiao Tong University "Medical and Research" Program (ZH2018ZDA04), Science and Technology Commission of Shanghai Municipality (18ZR1434200, 18140901500 and 19440760400), and Research Fund of State Key Laboratory of Tribology, Tsinghua University, China (SKLT2020C11).

Appendix A. Supplementary data

Supplementary data to this article can be found online at https://doi.org/10.1016/j.bioactmat.2021.03.022.

References

[1] J. Knoop, J. Dekker, J.P. Klein, M. Leeden, M. Esch, D. Reiding, R.E. Voorneman, M. Gerritsen, L.D. Roorda, M.P. Steultjens, W.F. Lems, Biomechanical factors and physical examination findings in osteoarthritis of the knee: associations with tissue abnormalities assessed by conventional radiography and high-resolution 3.0 Tesla magnetic resonance imaging, Arthritis Res. Ther. 14 (2012) R212.
[2] T.L. Vincent, Targeting mechanotransduction pathways in osteoarthritis: a focus on the pericellular matrix, Curr. Opin. Pharmacol. 13 (2013) 449–454.
[3] H. Zhang, L. Blunt, X. Jiang, L. Brown, S. Barrans, The significance of the micropores at the stem–cement interface in total hip replacement, J. Biomater. Sci. Polym. Ed. 22 (2011) 845–856.
[4] C. Cooper, J.Y. Reginster, B. Cortet, M. Diaz-Curiel, R.S. Lorenc, J.A. Kanis, R. Rizzoli, Long-term treatment of osteoporosis in postmenopausal women: a review from the European society for clinical and economic aspects of osteoporosis and osteoarthritis (ESCEO) and the international osteoporosis foundation (IOF), Curr. Med. Res. Opin. 28 (2012) 475–491.
[5] L. Kock, C.C. van Donkelaar, K. Ito, Tissue engineering of functional articular cartilage: the current status, Cell Tissue Res. 347 (2012) 613–627.
[6] Z. Unlu, K. Ay, C. Tuzun, Comparison of intra-articular tenoxicam and oral tenoxicam for pain and physical functioning in osteoarthritis of the knee, Clin. Rheumatol. 25 (2006) 54–61.
[7] T. Xin, J. Mao, L. Liu, J. Tang, L. Wu, X. Yu, Y. Gu, W. Cui, L. Chen, Programmed sustained release of recombinant human bone morphogenetic protein-2 and inorganic ion composite hydrogel as artificial periosteum, ACS Appl. Mater. Interfaces 12 (2020) 6840–6851.
[8] G. Zhong, J. Yao, X. Huang, Y. Luo, M. Wang, J. Han, F. Chen, Y. Yu, Injectable ECM hydrogel for delivery of BMSCs enabled full-thickness meniscus repair in an orthotopic rat model, Bioact. Mater. 5 (2020) 871–879.
[9] C. Fan, K. Xu, Y. Huang, S. Liu, T. Wang, W. Wang, W. Hu, L. Liu, M. Xing, S. Yang, Viscosity and degradation controlled injectable hydrogel for esophageal endoscopic submucosal dissection, Bioact. Mater. 6 (2021) 1150–1162.
[10] A. Tezel, G.H. Fredrickson, The science of hyaluronic acid dermal fillers, J. Cosmet. 10 (2009) 35–42.
[11] A. Sulistio, F.M. Mansfeld, F. Reyes-Ortega, A.M. D'Souza, S.M.Y. Ng, S. Birkett, A. Blencowe, G.G. Qiao, C.B. Little, C.C. Shu, A.M. Bendele, D. Valade, A. C. Donohue, J.F. Quinn, M.R. Whittaker, T.P. Davis, R.J. Tait, Intra-articular treatment of osteoarthritis with diclofenac-conjugated polymer reduces inflammation and pain, ACS Appl. Bio Mater. 2 (2019) 2822–2832.
[12] Y. Seong, G. Lin, B.J. Kim, H. Kim, S. Kim, S. Jeong, Hyaluronic acid-based hybrid hydrogel microspheres with enhanced structural stability and high injectability, ACS Omega 4 (2019) 13834–13844.
[13] P. Chen, C. Xia, S. Mei, J. Wang, Z. Shan, X. Lin, S. Fan, Intra-articular delivery of sinomenium encapsulated by chitosan microspheres and photo-crosslinked GelMA hydrogel ameliorates osteoarthritis by effectively regulating autophagy, Biomaterials 81 (2016) 1–13.
[14] Z. Zhang, G. Huang, Intra-articular lornoxicam loaded PLGA microspheres: enhanced therapeutic efficiency and decreased systemic toxicity in the treatment of osteoarthritis, Drug Deliv. 19 (2012) 255–263.
[15] P. Chen, C. Xia, S. Mei, J. Wang, Z. Shan, X. Lin, S. Fan, Intra-articular delivery of sinomenium encapsulated by chitosan microspheres and photo-crosslinked GelMA hydrogel ameliorates osteoarthritis by effectively regulating autophagy, Biomaterials 81 (2016) 1–13.
[16] J. Seror, L. Zhu, R. Goldberg, A.J. Day, J. Klein, Supramolecular synergy in the boundary lubrication of synovial joints, Nat. Commun. 6 (2015) 649.
[17] W. Wei, Y. Ma, X. Yao, W. Zhou, X. Wang, C. Li, J. Lin, Q. He, S. Leptihn, H. Ouyang, Advanced hydrogels for the repair of cartilage defects and regeneration, Bioact. Mater. 6 (2021) 998–1011.
[18] G. Liu, Z. Liu, N. Li, X. Wang, F. Zhou, W. Liu, Hairy polyelectrolyte brushes-grafted thermosensitive microgels as artificial synovial fluid for simultaneous biomimetic lubrication and arthritis treatment, ACS Appl. Mater. Interfaces 6 (2014) 20452–20463.
[19] J. Klein, Hydration lubrication, Friction 1 (2013) 1–23.

[20] C.J. Alexander, Idiopathic osteoarthritis: time to change paradigms, Skeletal Radiol. 33 (2004) 321–324.
[21] M. Tanaka, S. Kobayashi, D. Murakami, F. Aratsu, A. Kashiwazaki, T. Hoshiba, K. Fukushima, Design of polymeric biomaterials: the "intermediate water concept", Bull. Chem. Soc. Jpn. 92 (2019) 2043–2057.
[22] M. Kyomoto, T. Moro, S. Yamane, M. Hashimoto, Y. Takatori, K. Ishihara, Poly (ether-ether-ketone) orthopedic bearing surface modified by self-initiated surface grafting of poly(2-methacryloyloxyethyl phosphorylcholine), Biomaterials 34 (2013) 7829–7839.
[23] X. Ji, Y. Yan, T. Sun, Q. Zhang, Y. Wang, M. Zhang, H. Zhang, X. Zhao, Glucosamine sulphate-loaded distearoyl phosphocholine liposomes for osteoarthritis treatment: combination of sustained drug release and improved lubrication, Biomater. Sci. 7 (2019) 2716–2728.
[24] H. Lee, S.M. Dellatore, W.M. Miller, P.B. Messersmith, Mussel-inspired surface chemistry for multifunctional coatings, Science 318 (2007) 426–430.
[25] G. Pan, S. Sun, W. Zhang, R. Zhao, W. Cui, F. He, L. Huang, S.H. Lee, K.J. Shea, Q. Shi, H. Yang, Biomimetic design of mussel-derived bioactive peptides for dual-functionalization of titanium-based biomaterials, J. Am. Chem. Soc. 138 (2016) 15078–15086.
[26] F. Zhang, Q. Zhang, X.Y. Li, N. Huang, X. Zhao, Z.L. Yang, Mussel-inspired dopamine-Cu^{II} coatings for sustained in situ generation of nitric oxide for prevention of stent thrombosis and restenosis, Biomaterials 194 (2019) 117–129.
[27] Y. Jiao, S. Liu, Y. Sun, W. Yue, H. Zhang, Bioinspired surface functionalization of nanodiamonds for enhanced lubrication, Langmuir 34 (2018) 12436–12444.
[28] Y. Han, S. Liu, Y. Sun, Y. Gu, H. Zhang, Bioinspired surface functionalization of titanium for enhanced lubrication and sustained drug release, Langmuir 35 (2019) 6735–6741.
[29] L. Cheng, Y. Wang, G. Sun, S. Wen, L. Deng, H. Zhang, W. Cui, Hydration-enhanced lubricating electrospun nanofibrous membranes prevent tissue adhesion, Research 2020 (2020) 4907185.
[30] X. Zhao, S. Liu, L. Yildirimer, H. Zhao, R. Ding, H. Wang, W. Cui, D. Weitz, Injectable stem cell-laden photocrosslinkable microspheres fabricated using microfluidics for rapid generation of osteogenic tissue constructs, Adv. Funct. Mater. 26 (2016) 2809–2819.
[31] J. Wu, G. Li, T. Ye, G. Lu, R. Li, L. Deng, L. Wang, M. Cai, W. Cui, Stem cell-laden injectable hydrogel microspheres for cancellous bone regeneration, Chem. Eng. J. 393 (2020) 124715.
[32] Y. Yan, T. Sun, H. Zhang, X. Ji, Y. Sun, X. Zhao, L. Deng, J. Qi, W. Cui, H. Santos, H. Zhang, Euryale ferox seed-inspired superlubricated nanoparticles for treatment of osteoarthritis, Adv. Funct. Mater. 29 (2019) 1807559.
[33] H. Chen, T. Sun, Y. Yan, X. Ji, Y. Sun, X. Zhao, J. Qi, W. Cui, L. Deng, H. Zhang, Cartilage matrix-inspired biomimetic superlubricated nanospheres for treatment of osteoarthritis, Biomaterials 242 (2020) 119931.
[34] C. Li, K. Chen, H. Kang, Y. Yan, K. Liu, C. Guo, J. Qi, K. Yang, F. Wang, L. Guo, C. He, L. Deng, Double-stranded RNA released from damaged articular chondrocytes promotes cartilage degeneration via Toll-like receptor 3-interleukin-33 pathway, Cell Death Dis. 8 (2017) e3165.
[35] K.J. Livak, T.D. Schmittgen, Analysis of relative gene expression data using real-time quantitative PCR and the $2^{-\Delta\Delta CT}$ method, Methods 25 (2001) 402–408.
[36] K. Pritzker, S. Gay, S. Jimenez, K. Ostergaard, J. Pelletier, P. Revell, D. Salter, W. van den Berg, Osteoarthritis cartilage histopathology: grading and staging, Osteoarthritis Cartilage 14 (2006) 13–29.
[37] X.L. Tan, Y.L. Sun, T. Sun, H.Y. Zhang, Mechanised lubricating silica nanoparticles for on-command cargo release on simulated surfaces of joint cavities, Chem. Commun. 55 (2019) 2593–2596.
[38] Y.X. Wang, Y.L. Sun, Y.H. Gu, H.Y. Zhang, Articular cartilage-inspired surface functionalization for enhanced lubrication, Adv. Mater. Interfac. 6 (2019) 1900180.
[39] R. Zheng, J. Zhan, X. Wang, D. Kaplan, N. Pesika, V.T. John, Lubrication properties of phospholipid liposome coated silk microspheres, Part. Part. Syst. Char. 30 (2013) 133–137.
[40] O.M. Braun, Simple model of microscopic rolling friction, Phys. Rev. Lett. 95 (2005) 126104.
[41] W.W. Zhao, H. Wang, Y. Han, H.M. Wang, Y.L. Sun, H.Y. Zhang, Dopamine/phosphorylcholine copolymer as an efficient joint lubricant and ROS scavenger for the treatment of osteoarthritis, ACS Appl. Mater. Interfaces 12 (2020) 51236–51248.